Future Measurements of the Neutron Magnetic Form Factor (G_M^n) at Jefferson Lab

G.P. Gilfoyle
University of Richmond, Richmond, VA 23173

Outline

1. Motivation and Background
2. Approved JLab G_M^n Program
3. Compare and Contrast
4. Summary and Conclusions

Trento

Scientific Motivation - What We Hope to Learn.

- Elastic electromagnetic form factors (EEFFs) related to the distribution of charge and magnetization in the nucleon (Gerry Miller).
- Reveal the internal landscape of the nucleon and nuclei - limiting case for generalized parton distributions (Kroll, Kumericki).
- Required for flavor decomposition and mapping quark substructure (Bogdan, Cisbani).
- Early challenge for lattice QCD (Syritsyn).
- Part of a broad campaign to measure the four EEFFs at Jefferson Lab (Puckett, Franklin, Riordan, Annand, Sawatzky).
- Measuring G_M^n.
  - Neutron form factors (G_E^n, G_M^n) not as well known as the proton ones.
  - The magnetic form factors G_M needed to extract electric ones G_E from polarization transfer and double polarization asymmetry measurements.

Scientific Motivation - What We Hope to Learn.

- Elastic electromagnetic form factors (EEFFs) related to the distribution of charge and magnetization in the nucleon (Gerry Miller).
- Reveal the internal landscape of the nucleon and nuclei - limiting case for generalized parton distributions (Kroll, Kumericki).
- Required for flavor decomposition and mapping quark substructure (Bogdan, Cisbani).
- Early challenge for lattice QCD (Syritsyn).
- Part of a broad campaign to measure the four EEFFs at Jefferson Lab (Puckett, Franklin, Riordan, Annand, Sawatzky).
- Measuring G_M^n.
  - Neutron form factors (G_E^n, G_M^n) not as well known as the proton ones.
  - The magnetic form factors G_M needed to extract electric ones G_E from polarization transfer and double polarization asymmetry measurements.

EEFFs have played an essential role in nuclear and nucleon structure for more than a half century.

Some Necessary Background

- EEFFs cross section described with Dirac (F_1) and Pauli (F_2) form factors

$$\frac{d\sigma}{d\Omega} = \sigma_{Mott} \left[\left(F_1^2 + \kappa^2 \tau F_2^2 \right) + 2\tau \left(F_1 + \kappa F_2 \right)^2 \tan^2 \left(\frac{\theta_e}{2} \right) \right]$$

where

$$\sigma_{Mott} = \frac{\alpha^2 E' \cos^2(\frac{\theta_e}{2})}{4E^3 \sin^4(\frac{\theta_e}{2})}$$

and κ is the anomalous magnetic moment, E (E') is the incoming (outgoing) electron energy, θ is the scattered electron angle and $\tau = Q^2/4M^2$.

- For convenience use the Sachs form factors.

$$\frac{d\sigma}{d\Omega} = \sigma^n_{Mott} \left(\frac{(G^n_E)^2 + \tau (G^n_M)^2}{1+\tau} + 2\tau \tan^2 \frac{\theta_e}{2} (G^n_M)^2 \right) = \frac{\sigma_{Mott}}{\epsilon(1+\tau)} \left(\epsilon G_E^2 + \tau G_M^2 \right)$$

where

$$G_E = F_1 - \tau F_2 \quad \text{and} \quad G_M = F_1 + F_2 \quad \text{and} \quad \epsilon = \left[1 + 2(1+\tau) \tan^2 \frac{\theta_e}{2} \right]^{-1}$$

Where We Are Now.

- G_M^p reasonably well known over large Q^2 range.
- The ratio G_E^p/G_M^p from recoil polarization measurements diverged from previous Rosenbluth separations.
  - Two-photon exchange (TPE).
  - Effect of radiative corrections.
- Neutron magnetic FF G_M^n still follows dipole.
- High-Q^2 G_E^n opens up flavor decomposition.

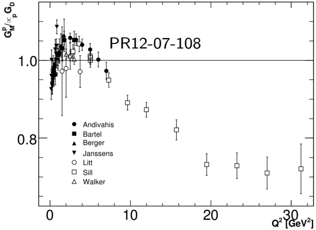

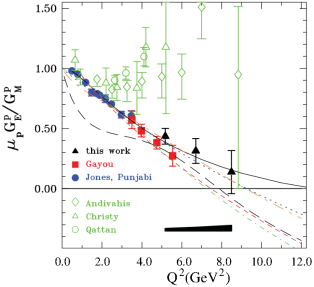

PRL **104**, 242301 (2010)

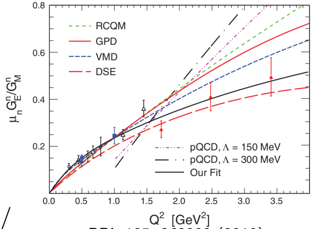

PRL 105, 262302 (2010)

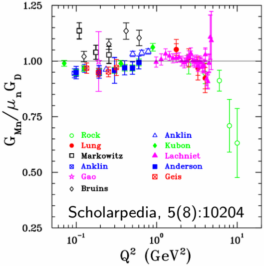

Scholarpedia, 5(8):10204

Where We Are Now.

- G_M^p reasonably well known over large Q^2 range.
- The ratio G_E^p/G_M^p from recoil polarization measurements diverged from previous Rosenbluth separations.
    - Two-photon exchange (TPE).
    - Effect of radiative corrections.
- Neutron magnetic FF G_M^n still follows dipole.
- High-Q^2 G_E^n opens up flavor decomposition.

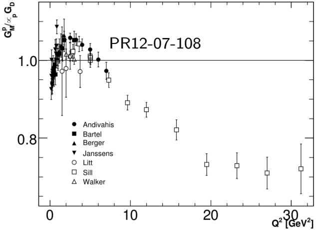

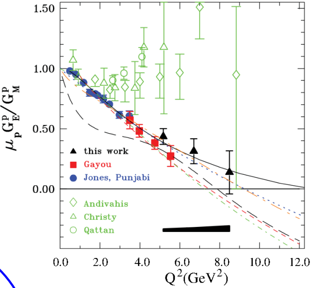

PRL **104**, 242301 (2010)

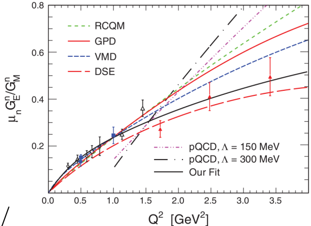

PRL 105, 262302 (2010)

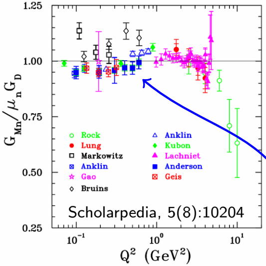

Scholarpedia, 5(8):10204

Tension among G_M^n measurements.

Tension in Low-Q^2 G_M^n measurements

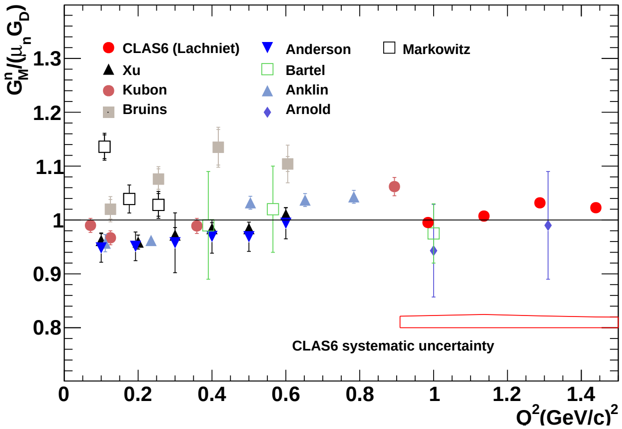

Experiments used ratio method unless noted otherwise.

Author	Reference	NDE Method	Author	Reference	NDE Method
Lachniet	PRL 102, 192001 (2009)	$^1H(e, e'\pi^+n)$	Anderson[1]	PRC 75, 034003 (2007)	NA
Xu[1]	PRC 67, 012201 (2003)	NA	Bartel	NP B58, 429 (1973)	$^1H(\gamma, \pi^+n)$
Kubon	PLB 524, 26 (2002)	$^1H(n, p)n$	Anklin	PLB 336, 313 (1998)	$^1H(n, p)n$
Arnold[2]	PRL 61, 806 (1988)	NA	Anklin	PLB 426, 248 (1998)	$^1H(n, p)n$
Bruins	PRL 75, 21 (1995)	$^1H(\gamma, \pi^+)n$	Markowitz[3]	PRC 48, R5, (1993)	$^2H(\gamma, np)$

1 - $^3\vec{He}(\vec{e}, e')$ 2 - $^2H(e, e')$ 3 - $^2H(e, e'n)$

Where We Are Going - New Experiments

The JLab Lineup

Quantity	Method	Target	$Q^2 (GeV^2)$	Hall	Beam Days
G_M^n	$E - p/e - n$ ratio	$LD_2 - LH_2$	$3.5 - 13.0$	B	30
G_M^n	$E - p/e - n$ ratio	LD_2, LH_2	$3.5 - 13.5$	A	25
G_M^p	Elastic scattering	LH_2	$7 - 15.5$	A	24
G_E^p/G_M^p	Polarization transfer	LH_2	$5 - 12$	A	45
G_E^n/G_M^n	Double polarization asymmetry	polarized ^{3}He	$5 - 8$	A	50
G_E^n/G_M^n	Polarization transfer	LD_2	$4 - 7$	C	50

All experiments build on successful ones from the 6-GeV era.

Why two for G_M^n?

'... the PAC is convinced that proposed measurement is very valuable to determine the magnetic form factor with high precision. Both experiments using different equipment, this will allow a better control for the systematic error on GM(n) - '

- PAC34 Report on Hall A G_M^n.

How We Will Get There: Jefferson Lab

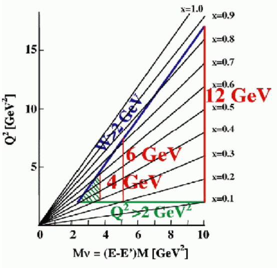

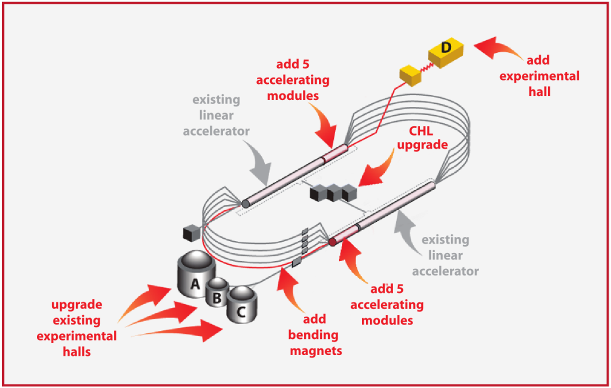

Continuous Electron Beam Accelerator Facility (CEBAF)

- Superconducting Electron Accelerator (338 cavities), 100% duty cycle.
- $E_{max} = 11\ \mathrm{GeV}$ (Halls A, B, and C) and $12\ \mathrm{GeV}$ (Hall D), $\Delta E/E \approx 2 \times 10^{-4}$, $I_{summed} \approx 90\ \mu A$, $P_e \geq 80\%$.

The Experiments - New Detectors

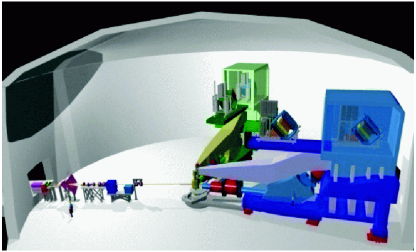

Hall A - High Resolution Spectrometer (HRS) pair, SuperBigBite (SBS), neutron detector, and specialized installation experiments.

E12-09-019 (Quinn, Wojtsekhowski, Gilman)

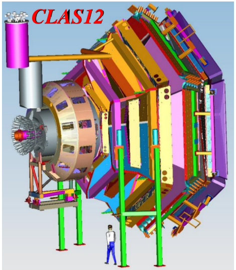

Hall B - CLAS12 large acceptance spectrometer operating at high luminosity with toroid (forward detector) and solenoid (central detector).

E12-07-104 (Gilfoyle, Hafidi, Brooks)

The Experiments - Detector Summaries

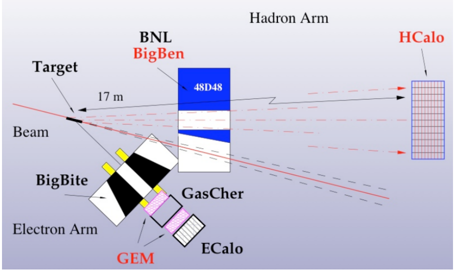

SBS - 2-3 Tesla*m magnet, solid angle 70 msr at 15 deg, GEM chambers (70 m resolution), $\Delta p/p \approx 0.5\%$, $\Delta\theta \approx 0.5\ mr$, open geometry, small hadron angles accessible, can sustain high luminosity running.

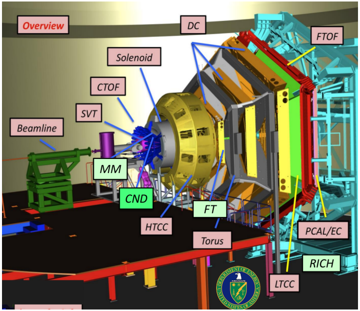

Hall B - Large acceptance with toroidal magnet ($B_{max} \approx 3.5\ T$) and solenoid ($B_{center} \approx 5\ T$) with multiple systems (drift chambers, calorimeters, TOF, Cherenkov, vertex trackers) for particle identification and tracking ($\Delta p/p \approx 1\%$).

The G_M^n Measurement - Ratio Method on Deuterium

- Use deuterium as a neutron target.
- Same method used by both Hall A and Hall B experiments.
- Simultaneously measure $e-p$ and $e-n$ events in quasi-elastic (QE) kinematics.
- Ratio Method on Deuterium:

$$R = \frac{\frac{d\sigma}{d\Omega}[^2\mathrm{H}(e,e'n)_{QE}]}{\frac{d\sigma}{d\Omega}[^2\mathrm{H}(e,e'p)_{QE}]} = a \times \frac{\sigma^n_{Mott}\left(\frac{(G_E^n)^2+\tau(G_M^n)^2}{1+\tau} + 2\tau\tan^2\frac{\theta_e}{2}(G_M^n)^2\right)}{\frac{d\sigma}{d\Omega}[^1\mathrm{H}(e,e')p]}$$

  where a is nuclear correction close to one. So

$$G_M^n = \pm\sqrt{\left[R\frac{\frac{d\sigma}{d\Omega}[^1\mathrm{H}(e,e')p](1+\tau_n)}{a\sigma^n_{Mott}} - G_E^{n\,2}\right]\frac{\epsilon_n}{\tau_n}}$$

- Reduces sensitivity to changes in running conditions, nuclear effects, radiative corrections, Fermi motion corrections.
- Take advantage of the experience from CLAS6 measurement of G_M^n.

The G_M^n Measurement - Running Conditions

Hall A

- QE kinematics.
- Electron arm: ECal (SBS).
- Hadron arm: HCal (SBS) with BigBen dipole.
- Kinematics: $\mathrm{Q}^2 = 3.5 - 13.5\ (\mathrm{GeV/c})^2$.
- Beamtime: 25 days.
- When?: 2019

Hall B

- QE kinematics.
- Electrons, protons: CLAS12 forward detector.
- Neutrons: forward Time-of-Flight (FTOF) AND calorimeters (PCAL/EC).
- Kinematics: $\mathrm{Q}^2 = 3.5 - 13.0\ (\mathrm{GeV/c})^2$.
- Beamtime: 30 days.
- When?: First runs in 2018.

Precise measurement of the neutron detection efficiency (NDE) is needed for both.

Proton/Neutron Selection

Hall A

- Use BigBen to deflect protons vertically to separate QE neutrons and protons at the 95% level.
- Remaining 5% can be estimated using HCal veto or event topology.
- Use cut on θ_{pq}, angle between $\vec{q}$ and $\vec{p}_N$, to reduce inelastic contamination.
- W^2 cut to remove high-W^2 inelastics.

Hall B

- Use CLAS12 toroid to deflect protons to separate QE protons and neutrons.
- Use cut on θ_{pq}, angle between $\vec{q}$ and $\vec{p}_N$, to reduce inelastic contamination.
- Veto event if additional tracks are observed (hermiticity cut).
- W^2 cut to remove high-W^2 inelastics.

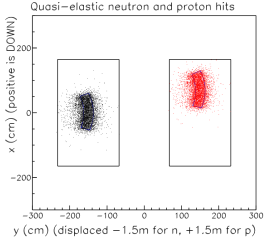

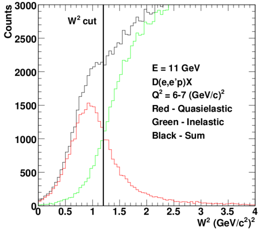

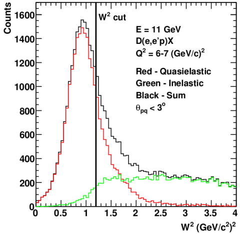

An Angular Constraint to Select QE Events

- The angle θ_{pq} is between the transferred 3-momentum $\vec{q}$ and the momentum $\vec{p}_N$ of the detected nucleon.
- In quasielastic interactions on nuclei, the ejected nucleon comes out in a direction close to the 3-momentum transfer direction $\vec{q}$.
- The internal Fermi motion and final-state interaction (FSI) smears the momentum of the ejected nucleon in a cone around $\vec{q}$.
- The inelastic maximum is at a larger angle.
- These features enable one to separate QE events from inelastic ones.

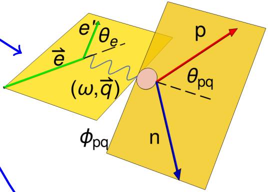

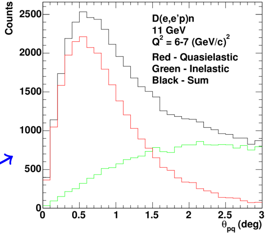

An Angular Constraint to Select QE Events

- The angle θ_{pq} is between the transferred 3-momentum $\vec{q}$ and the momentum $\vec{p}_N$ of the detected nucleon.
- In quasielastic interactions on nuclei, the ejected nucleon comes out in a direction close to the 3-momentum transfer direction $\vec{q}$.
- The internal Fermi motion and final-state interaction (FSI) smears the momentum of the ejected nucleon in a cone around $\vec{q}$.
- The inelastic maximum is at a larger angle.
- These features enable one to separate QE events from inelastic ones.

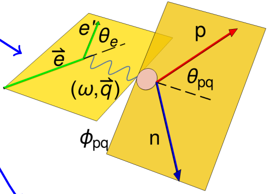

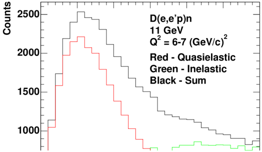

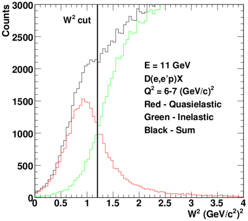

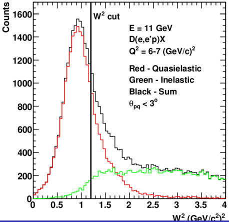

Using θ_{pq} Cut to Reduce Inelastic Background

- Hall A: At higher Q^2 the QE peak gets wider and overlaps more with inelastic processes. Use cut on θ_{pq} to suppress inelastic background.

Effect of θ_{pq} cut and higher Q^2.

Good statistical precision in Hall A.

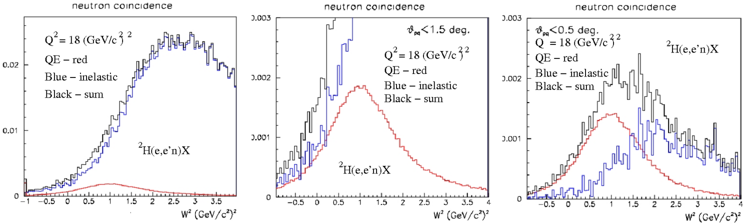

- Hall B: Same method can be applied in CLAS12.

Effect of θ_{pq} cut (worst case).

Unrealistic statistics to show effect.

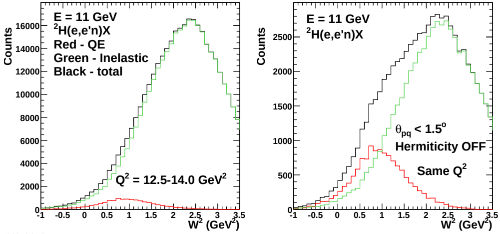

Proton/Neutron Selection

Hall A

- Use BigBen to deflect protons vertically to separate QE neutrons and protons at the 95% level.
- Remaining 5% can be estimated using HCal veto or event topology.
- Use cut on θ_{pq}, angle between $\vec{q}$ and $\vec{p}_N$, to reduce inelastic contamination.
- W^2 cut to remove high-W^2 inelastics.

Hall B

- Use CLAS12 toroid to deflect protons to separate QE protons and neutrons.
- Use cut on θ_{pq}, angle between $\vec{q}$ and $\vec{p}_N$, to reduce inelastic contamination.
- Veto event if additional tracks are observed (hermiticity cut).
- W^2 cut to remove high-W^2 inelastics.

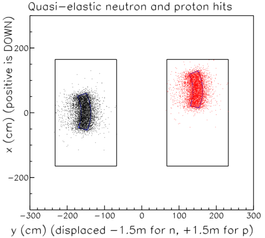

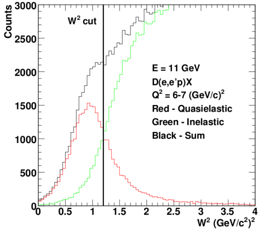

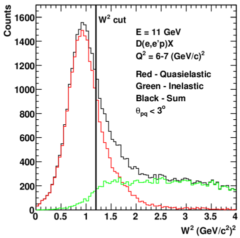

Hermiticity Cut to Reduce Inelastic Background in CLAS12

- Hall B: At higher Q^2 the QE peak gets wider and overlaps more with inelastic processes. Many inelastic $e - n$ and $e - p$ events actually have other particles associated with them.
- Use CLAS12 large acceptance to veto unwanted topologies (hermiticity cut) in addition to θ_{pq} cut. In other words require $e - n$ or $e - p$ tracks and nothing else.

Effect of θ_{pq} and hermiticity cuts.

Unrealistic statistics to show effect.

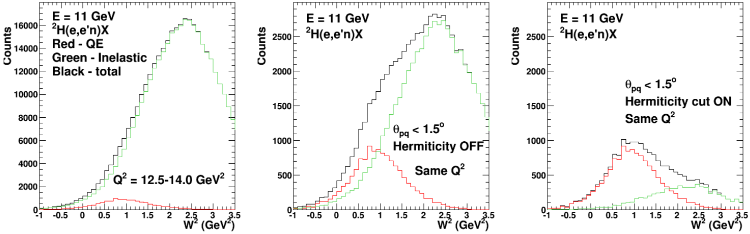

Hermiticity Cut to Reduce Inelastic Background in CLAS12

- Hall B: At higher Q^2 the QE peak gets wider and overlaps more with inelastic processes. Many inelastic $e-n$ a… y have other particles associated with them.
- Use CLAS12 large acceptance to veto unw… (hermiticity cut) in addition to θ_{pq} cut. In … $-\ n$ or $e-p$ tracks and nothing else.

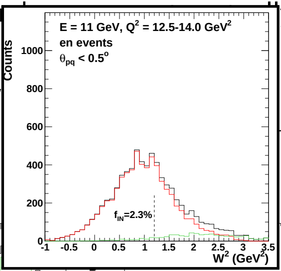

Effect of θ_{pq} and hermiticity cuts.

Unrealistic statistics to show effect.

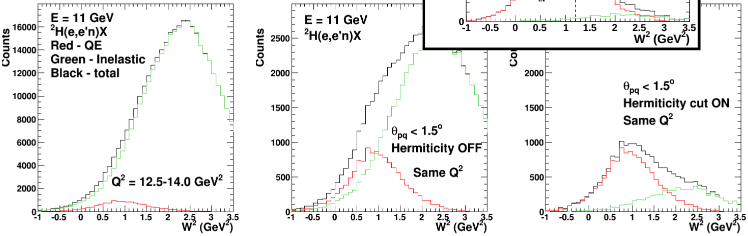

Acceptance Matching

- Use the measured electron information to predict the trajectory of the associated QE proton and neutron (yes, both).
- Swim the predicted neutron and proton tracks through CLAS12.
- Check that both hadron tracks strike the fiducial volume of CLAS12.
- If both strike CLAS12 continue the analysis, otherwise throw it out.

$e - p$ event

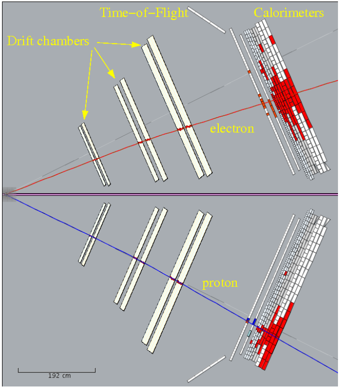

$e - n$ event

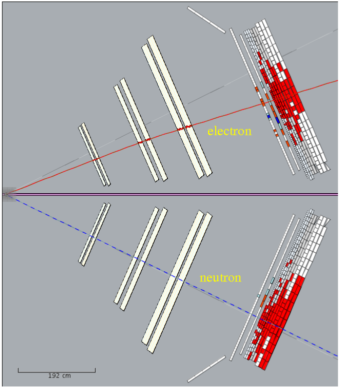

Measuring Proton Detection Efficiency

- Hall A: Measure $ep \rightarrow e'p$ elastic scattering on LH_2 calibration target.
- Use electron information to tag proton location in HCal (reconstructed nucleons).
- Proton detection efficiency is ratio of found protons to reconstructed.
- Use kinematic separation between elastics and pion threshold.

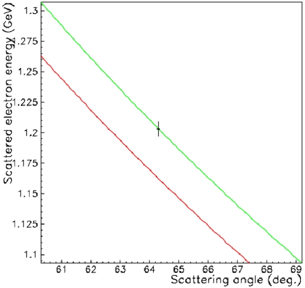

- Hall B: Use similar method to Hall A with dual-cell LH_2-LD_2 target.
- Dual-cell target provides *in-situ* calibration under production running conditions.

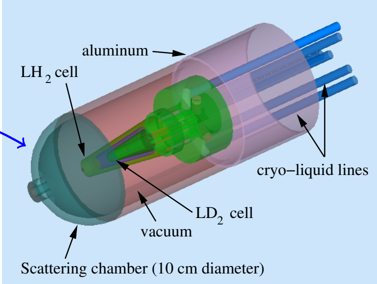

Measuring Neutron Detection Efficiency in Hall A

- Insert copper radiator in front of LH_2 proton target to produce bremsstrahlung photon beam.
- Use $p(\gamma, \pi^+)n$ as source of tagged neutrons - detect π^+ in HRS and tag neutron expected in HCal (reconstructed neutron).
- Select π^+ using end-point method. Suppress lower-momentum π^+'s from three-body interactions by requiring p_{π^+} exceed upper limit by 1.5% (SBS has 0.5% resolution.)
- Neutron detection efficiency (NDE) is ratio of observed neutrons (found neutrons) to reconstructed.
- Events from $p(e, \pi^+)$ will contribute a relatively small background that can be studied with the radiator removed.
- Good match to kinematics of the production reaction.
- Expect $\lesssim 2\%$ contribution to the systematic uncertainty from the neutron detection efficiency.

Measuring Neutron Detection Efficiency in Hall B

- Use proton target in dual-cell cryo-target for *in-situ* NDE measurement under running conditions.
- Measure $ep \to e'\pi^+ n$ from LH_2 cell to make tagged neutrons in the TOF and calorimeter.
- Detect electrons and π^+ in CLAS12 forward detector.
- Select neutrons with missing mass cut on $ep \to e\pi^+ X$.
- Use $e'\pi^+$ information to tag neutron location (reconstructed neutron).
- NDE is ratio of found neutrons to reconstructed ones.
- CLAS6 G_M^n results. Simulation results for CLAS12 are shown in the inset. CLAS12 measurement is at higher momentum where the efficiency is stable.

Calorimeter efficiency

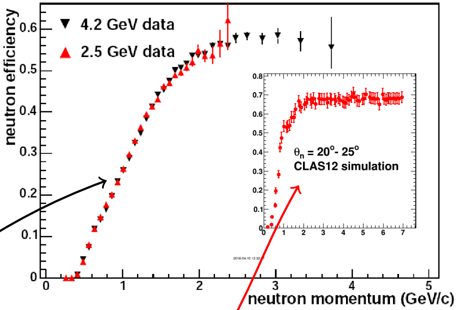

Systematic Uncertainties (%)

Hall A (at 13.5 $(\mathrm{GeV/c^2})^2$)

Quantity	$\Delta R/R$
HCal calibration	2.0
proton σ	1.7
Inelastic contamination	3.24
accidentals	< 0.07
Nucleon mis-identification	0.5
Nuclear Corrections	< 0.2
G_E^n	0.38
Target windows	0.2
Acceptance losses	0.1
Radiative corrections	< 0.2

$\Delta G_M^n/G_M^n$	2.1

Hall B (maximum values)

Quantity	$\Delta R/R$
Neutron efficiency	< 0.7
proton σ	< 1.5
Background subtraction	< 1.0
neutron accidentals	< 0.3
neutron proximity cut	< 0.2
Nuclear Corrections	< 0.2
G_E^n	< 0.7
θ_{pq} cut	< 1.0
Fermi loss correction	< 0.9
Neutron MM cut	< 0.5
proton efficiency	< 0.4
Radiative corrections	< 0.2

$\Delta G_M^n/G_M^n$	3.1

Anticipated Results

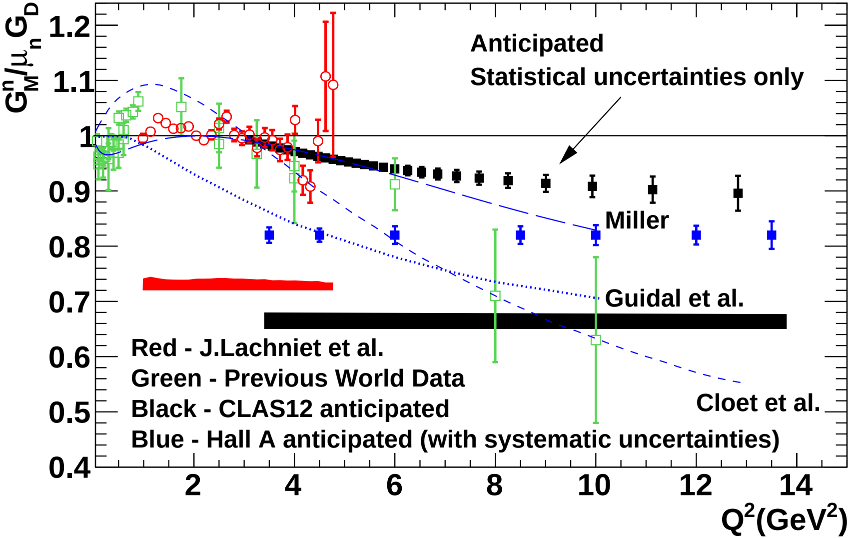

Consistency Checks

- Large overlap between Hall A and CLAS12 experiments.
- Large overlap with CLAS6 experiment using the same techniques.
- Internal consistency check in CLAS12 experiment between $e - n$ measured with calorimeters and forward time-of-flight system.

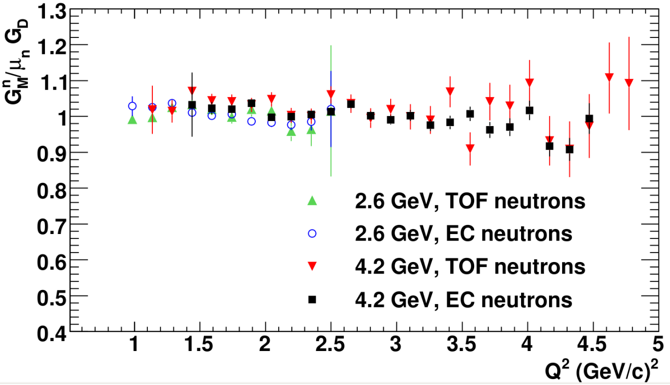

Comparison of Hall A and B Uncertainties

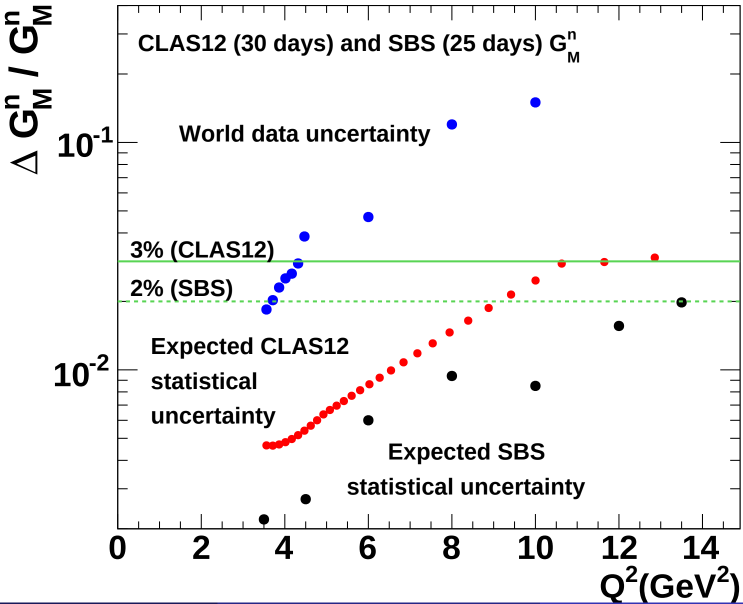

Summary and Conclusions

- Two experiments in Halls A and B will be devoted to the neutron magnetic form factor G_M^n.
- Both experiments will cover similar Q^2 ranges and more than double the range of high-precision measurements of G_M^n.
- Important consistency checks in both experiments.
- The high-luminosity Hall A measurement will have excellent statistical precision at all ${}^2\mathrm{Q}$.
- The hermiticity cut in the Hall B experiment will reduce the inelastic background to produce a cleaner QE signal.
- High-luminosity of SBS will enable higher Q^2 measurements in Hall A.

Additional Slides

CLAS12 Run Group Schedule - Tentative

Run Group	Days	2015	2016	2017	2018	2019	2020	2021	Remain
All Run Groups	**936**		CND	FT RICH MM			Trans. PT	**525**	**411**
HPS	180*	2-3	7 ?						
PRad	15*		10 ?						---
CLAS12 KPP 				**15**					
RG-A (proton)	139*			20 **50**					69*
RG-F (BoNuS)	42*				**40**				2
RG-B (deut.)	90*				**45**				45*
RG-C (NH_3)	120				**15**	**45**			60
RG-C-b (ND_3)	65					**35**			30
RG-E (Hadr.)	60					**20**	**15**		25
RG-G (TT)	110*						**55**		55
RG-D (CT)	60						**30**		30
RG-K (LiD)	55							**55**	---

Nuclear Corrections

- The factor $a(\mathrm{Q}^2)$ was calculated by Jeschonnek (Phys. Rev. C, 62 044613, 2000) for the CLAS12 kinematics and found to differ by less than 0.001 from unity.
- Two similar calculations for CLAS6 by Jeschonnek and by Arenhoeval differed from one by less than 0.003.
- For the Hall A proposal the cross section was calculated using PWIA for $1.0 < \mathrm{Q}^2 < 5\ (\mathrm{GeV}/\mathrm{c}^2)^2$, the AV18 deuteron wave function (R. Wiringa et al., Phys. Rev. C 51, 38, 1995) and Glauber theory for final-state interactions (FSI). Ratio of PWIA-only to full calculation with FSI differed by less than 0.001.
- Nuclear corrections associated with Fermi motion were calculated with the same code and showed effect less than 0.005.

Two-Photon Effects

- TPE corrections effect numerator and denominator.

$$R = a \times \frac{\sigma^n_{Mott}\left(\frac{(G^n_E)^2+\tau_n(G^n_M)^2}{1+\tau_n} + 2\tau_n \tan^2\frac{\theta_e}{2}(G^n_M)^2\right)}{\sigma^p_{Mott}\left(\frac{(G^p_E)^2+\tau_p(G^p_M)^2}{1+\tau_p} + 2\tau_p \tan^2\frac{\theta_e}{2}(G^p_M)^2\right)} \frac{1+\delta_n}{1+\delta_p}$$

- May not cancel in the ratio. Blunden *et al.*, PRC 72 034612 (2005) found $\delta_n - \delta_p \lesssim 0.02$.

Radiative Corrections

- Calculated for exclusive $D(e, e'p)n$ with the code EXCLURAD by Afanasev and Gilfoyle (CLAS-Note 2005-022). The ratio of the correction factors for $e - n/e - p$ events is close to unity.

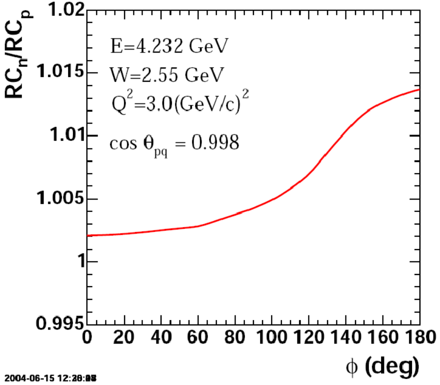

Optimizing θ_{pq} Cut

1. Recall effect of requiring $\theta_{pq} < 1.5^\circ$ and hermiticity cut to reduce inelastic background.

Effect of θ_{pq} and hermiticity cuts.

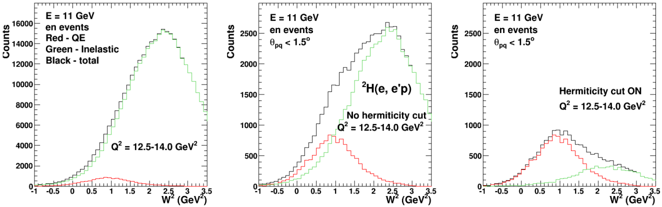

2. To reduce inelastic background further, reduce the maximum θ_{pq}.

$f_{IN} = \frac{inelastic}{total}$ for $W^2 < 1.2\ \mathrm{GeV}^2$.

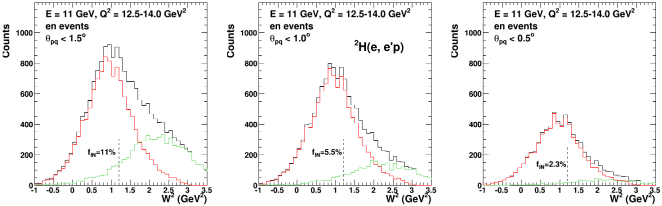

Hermiticity Cut

1. For the CLAS6 data, the hermiticity cut is not needed. Applying it just reduces the already small inelastic background (compare black and red histograms).
2. Without requiring $\theta_{pq} < 3^\circ$, the hermiticity cut still reduces the inelastic background (compare blue and green histograms).
3. Hermiticity cut here includes *ep* events with additional out-of-time tracks or ones that fall outside the vertex cut (1.5 cm).

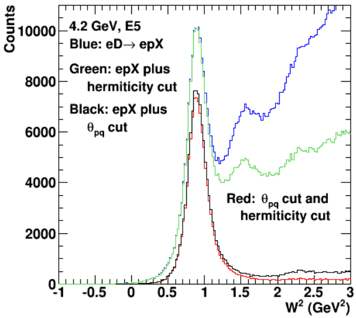

4. Effect of hermiticity cut in CLAS12 simulation is qualitatively consistent with CLAS6, E5 data.

Neutron Detection Efficiency Uncertainty

- Characterize the neutron detection efficiency ϵ_n with

$$\epsilon_n = S \times \left(1 - \frac{1}{1 + \exp(\frac{p_n - p_0}{a_0})}\right)$$

  where S is the height of the plateau for $p_n > 2\ GeV/c$, p_0 is the center of the rising part of ϵ_n, and a_0 controls the slope of ϵ_n in this region.
- Fit the ϵ_n with a third-order polynomial and a flat region.
- Use the original ϵ_n and the fit in reconstructing the neutrons and take the difference.

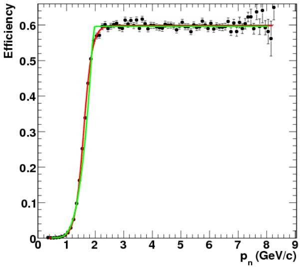

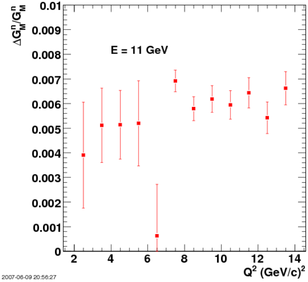

Tension in Low-Q^2 G_M^n measurements

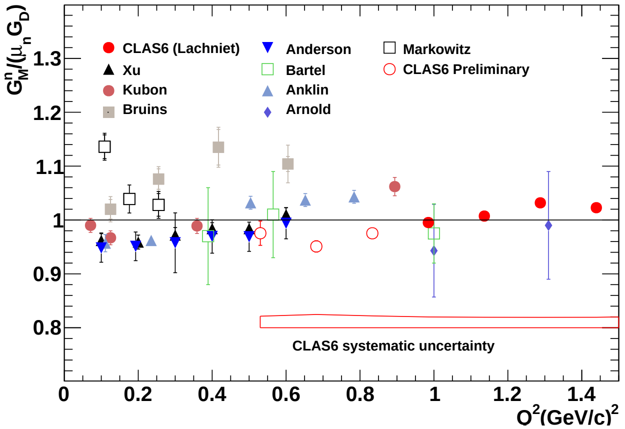

Experiments used ratio method unless noted otherwise.

Author	Reference	NDE Method	Author	Reference	NDE Method
Lachniet	PRL 102, 192001 (2009)	$^1\mathrm{H}(e, e'\pi^+ n)$	Anderson[1]	PRC 75, 034003 (2007)	NA
Xu[1]	PRC 67, 012201 (2003)	NA	Bartel	NP B58, 429 (1973)	$^1\mathrm{H}(\gamma, \pi^+ n)$
Kubon	PLB 524, 26 (2002)	$^1\mathrm{H}(n, p)n$	Anklin	PLB 336, 313 (1998)	$^1\mathrm{H}(n, p)n$
Arnold[2]	PRL 61, 806 (1988)	NA	Anklin	PLB 426, 248 (1998)	$^1\mathrm{H}(n, p)n$
Bruins	PRL 75, 21 (1995)	$^1\mathrm{H}(\gamma, \pi^+)n$	Markowitz[3]	PRC 48, R5, (1993)	$^2\mathrm{H}(\gamma, np)$

1 - $^3\vec{\mathrm{He}}(\vec{e}, e')$ 2 - $^2\mathrm{H}(e, e')$ 3 - $^2\mathrm{H}(e, e'n)$